PAPER

Study of glass transition temperature (T_g) of novel stress-sensitive composites using molecular dynamic simulation

IOP Publishing Modelling and Simulation in Materials Science and Engineering

Modelling Simul. Mater. Sci. Eng. **22** (2014) 065018 (13pp) doi:10.1088/0965-0393/22/6/065018

Study of glass transition temperature (T_g) of novel stress-sensitive composites using molecular dynamic simulation

B Koo, Y Liu, J Zou, A Chattopadhyay and L L Dai

School for Engineering of Matter, Transport, and Energy, Arizona State University, Tempe, AZ, 85287, USA

E-mail: Bonsung.Koo@asu.edu

Received 23 December 2013, revised 18 July 2014
Accepted for publication 21 July 2014
Published 19 August 2014

Abstract

This study investigates the glass transition temperature (T_g) of novel stress-sensitive composites capable of detecting a damage precursor using molecular dynamics (MD) simulations. The molecular structures of a cross-linked epoxy network (which consist of epoxy resin, hardener and stress-sensitive material) have been simulated and experimentally validated. The chemical constituents of the molecular structures are di-glycidyl ether of bisphenol F (DGEBF: epoxy resin), di-ethylene tri-amine (DETA: hardener) and tris-(cinnamoyloxymethyl)-ethane (TCE: stress-sensitive material). The cross-linking degree is varied by manipulating the number of covalent bonds through tuning a cutoff distance between activated DGEBF and DETA during the non-equilibrium MD simulation. A relationship between the cross-linking degree and T_gs has been studied numerically. In order to validate a proposed MD simulation framework, MD-predicted T_gs of materials used in this study have been compared to the experimental results obtained by the differential scanning calorimetry (DSC). Two molecular models have been constructed for comparative study: (i) neat epoxy (epoxy resin with hardener) and (ii) smart polymer (neat epoxy with stress-sensitive material). The predicted T_gs show close agreement with the DSC results.

Keywords: molecular dynamics, thermosetting polymer, mechanophore, cross-linking degree, glass transition temperature

(Some figures may appear in colour only in the online journal)

1. Introduction

There are limited materials that are 'intelligently' responsive to stress, although all materials deform under external stress and eventually exhibit fracture and failure. Recently, several stress-sensitive materials called mechanophore have been developed. As mechanophore activation is based on covalent bond-breaking that is induced by external stimuli, material-level damage detections have become possible. Spiropyran-based mechanophore was used in Davis *et al* [1], which consisted of carbon–oxygen covalent bonds forming colorless spiropyran. As the colorless spiropyran-based mechanophore is elongated, the colorless material becomes red because of the rupture of the carbon–oxygen covalent bond, resulting in a merocyanine structure. Recently, bis(adamantly)-1,2-dioxetane and polydiacetylenes have been discovered as mechanophore [2]. Another type of mechanophore, called cyclobutane, was reported in Cho *et al* [3]. Cyclobutane-based mechanophore consisting of carbon–carbon covalent bonds is transformed into cinnamate groups; these create green fluorescence emissions by breaking the carbon–carbon covalent bond. The feasibility of a novel self-sensing technique by embedding cyclobutane-based mechanophore material in a polymer matrix is currently being investigated by the authors [4]. In this paper, tris-(cinnamoyl oxymethyl)-ethane (TCE) is selected to construct the cyclobutane-based mechanophore. For simplicity, the cyclobutane-based mechanophore is called 'smart material'. Although these 'smart' materials offer novel sensing capability, it is important to develop a comprehensive understanding of the interactions between the smart material and the polymer matrix at the material level. This must include, but are not limited to, considering the effects of the smart material on both local and global scales. On the local scale, the changes in mechanical/thermal properties of the polymer matrix must be investigated. Likewise, the effect of the local scale changes on the polymer matrix composite material should be demonstrated on the global scale. As a fundamental investigation for understanding the local scale property of the smart material-embedded polymer matrix composite, this paper focuses on the glass transition temperature (T_g), which is the most critical thermal property.

A significant amount of work has been reported on the experimental characterization and fabrication of multifunctional composites. However, the determination of material properties through testing is labor intensive and expensive. For the last decade, many molecular dynamics simulations on epoxy-based systems, especially thermosetting polymer, have been reported. A majority of the research was based on the epoxy resin DGEBF (di-glycidyl ether of bisphenol F) with different hardeners such as DETDA [5–10], TETA [11–13], IPD (isophorane diamine) [14], DDS (diaminodiphenyl sulfone) [15], MDA (methylene dianilne) [16] and POP (polyoxypropylene diamines) [17]. The previously mentioned papers predicted T_gs and compared their estimates with experimental results. Likewise, in this paper, MD simulations and experiments are used to investigate T_gs of neat epoxy and smart polymer. While MD framework used in the literature estimates the cross-linking degree by comparing the predicted T_gs and the empirically/theoretically obtained relationship between T_gs and the cross-linking degree, the novelty of our MD simulation is the incorporation of a statistical step for predicting at cross-linking degree of epoxy-based system. The statistical step requires accurate force field information only and therefore could be very useful, especially when there is no reported literature about the target material's characteristics. The accuracy of the MD framework is established via experimental validations and the mechanical/thermal properties of the integrated epoxy and smart material system (referred to as 'smart polymer' in this paper). The estimated T_gs of the neat epoxy and smart polymer are compared with the experimental results obtained by the differential scanning calorimetry (DSC).

Several force fields have been developed for the MD simulation of epoxy-based systems. As both interatomic and intermolecular potential are very critical in epoxy-based systems, all-atom force fields are considered instead of united-atom force fields to increase the accuracy of MD simulation results (despite computational expense). Assisted model building with energy refinement (AMBER) was developed for modeling biomolecules and organic materials. Lin *et al* [18–20] used AMBER for an epoxy network consisting of DGEBA and TMAB. The Dreiding force field is a much more general force field than other force fields, but it is effectively used for protein and polymer simulations. Li *et al* [21] used the Dreiding force field for the DGEBA and 33DDS atomistic simulations. One of the famous force fields in organic research is the Chemistry at HARvard Macromolecular Mechanics (CHARMM) [22]. Similarly, Optimized Potential for Liquid Simulation (OPLS) has been developed for peptide research. Valavala *et al* [10] and Bandyopadhyay *et al* [9] used OPLS for the atomistic simulation of DGEBF and DETDA. Condensed-phase optimized molecular potentials for atomistic simulation studies (COMPASS) has been used for polymer research, and many epoxy-based MD simulations have been conducted with various epoxy resin and hardener [5, 11–13, 15, 23]. As mentioned earlier, various force fields have been used and developed; however, the best force field for epoxy-based systems has not yet been clearly addressed. This is because the force field decision is highly dependent on the material. The Merck molecular force field (MMFF), which was developed for general organic research and pharmaceutical development that requires the most accurate results, is used for the epoxy-based systems used in this paper [24–28]. Using MMFF, experimental T_gs were reproduced within 2% error tolerance. Details are discussed in section 2.

In this paper, the validation of the proposed MD simulation framework and predictions of T_gs of both neat epoxy and smart polymer are investigated. Taking into account the chemical curing process of epoxy resin and hardener, the carbon–nitrogen covalent bond generation is implemented numerically. Based on the numerical method for covalent bond generation, the cross-linking degree estimations of epoxy-based system are conducted using a stochastic method, which makes the MD simulation results more reliable. The MD simulation is also used to investigate the relationship between the cross-linking degree and T_gs.

2. Molecular dynamics simulation and experimental validation

An MD-simulation-based approach is developed to characterize the nonlinear properties of the smart material (mechanophore) at the molecular level. Although the mechanophore activation study is not the focus of this paper, a brief description of the smart material is provided for completeness. TCE monomer is used to form a TCE polymer comprising cyclobutane-structure, which is photosynthesized by ultra-violet (UV) irradiation (330–380 nm wavelength). Physical discontinuities break the cyclobutane-structure in TCE polymer and the polymer reverts back to a TCE monomer, which consists of cinnamoly groups. The cinnamoly groups then emit fluorescence (540–560 nm wavelengths) by UV excitation. It is important to note that the smart material is activated at the molecular level by covalent bond dissociation upon mechanical loading and is tangled with epoxy resin/hardener at the same level. The entangled structure critically affects the activation of mechanophore as it distributes the external energy in the system. Since the entangled structure is determined at the curing process, it is necessary to model the cured epoxy system in MD simulations by emulating the chemical covalent bonds that generate network structure and play a very important role in epoxy-based systems. Besides the numerical generation of a covalent bond, the stochastic method is used to estimate the cross-linking degree of the cured epoxy system; this leads to more reliable results from MD simulations. MMFF, one of the all-atom force fields, is used to address

Table 1. Components of smart polymer (100 : 27 and 10% TCE).

	Weight	Formula	# of molecules
DGEBF	313 g mol^{-1}	$C_{19}H_{20}O_4$	65
DETA	103 g mol^{-1}	$C_4H_{13}N_3$	55
TCE	510 g mol^{-1}	$C_{32}H_{30}O_6$	5

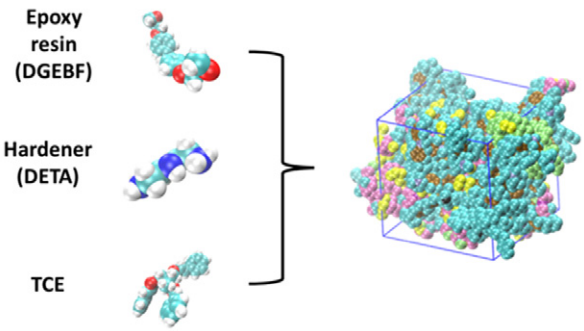

Figure 1. Schematic illustration of a smart polymer unit cell.

the inter/intra-molecular potential energy of the neat epoxy and smart polymer. All of the MD simulations have been performed with Large-scale atomic molecular massively parallel simulator (LAMMPS) in conjunction with MMFF [29].

2.1. Configuration of unit cell and force field

For MD simulations based on an all-atom force field, atomistic molecular structures of each component in an objective system should be defined. This study used commercial products of epoxy resin (FS-A23) and hardener (FS-B412), which was used for manufacturing carbon-fiber-reinforced composites [30]. Molecular structures of DGEBF and DETA are used to construct neat epoxy unit cells for MD simulations. A well-mixed, epoxy-based system is guaranteed through the distribution of all the molecules randomly in each unit cell without overlap. The number of molecules is determined by the weight ratio 100 : 27 (DGEBF : DETA) which is used for making experimental samples in this study. The weight of the TCE is 10% of the total weight of the neat epoxy unit cell. Table 1 and figure 1 show the calculated number of molecules and three-dimensional (3D) molecular structures in the smart polymer unit cell (4235 atoms).

The force field MMFF, which is derived from computational data based on *ab initio* calculations, can accurately reproduce experimental results in chemical and pharmaceutical research [31–33]. This has been validated by chemists and crystallographers [24–28]. The experimental data is maintained by the Cambridge Crystallography Data Centre (CCDC), a major international resource for chemical and pharmaceutical research [34]. Based on MMFF, topologies and force field parameters of all the molecules used in MD simulations are generated by a web-based molecular structure generator, which is supported by the Swiss Institute of Bioinformatics (SIB)—an international research foundation providing organic chemistry resources [35]. The MMFF force field is used in conjunction to LAMMPS, which has versatile features such as bond breaking/formation, unit cell deformation, and the ability to create/delete atoms. It is worth noting that although LAMMPS does not support MMFF, this study is able

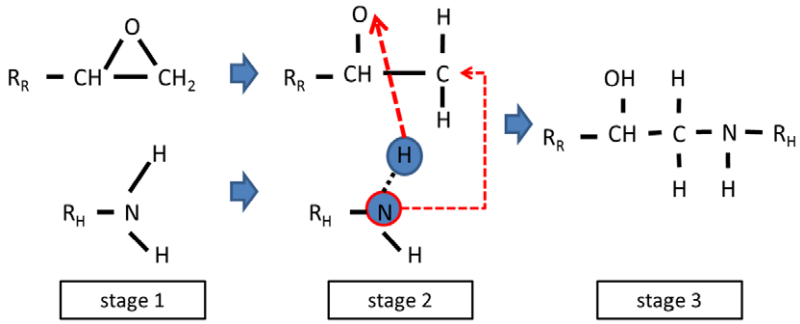

Figure 2. Procedure for covalent bond generation, where R_R is the remaining part of the resin, R_H is the remaining part of the hardener, C, N, H and O are carbon, nitrogen, hydrogen and oxygen atoms, respectively.

to use MMFF in LAMMPS due to functional forms generated by SIB that are compatible with CHARMM force field, which is available in LAMMPS.

2.2. Numerical implementation of curing process

In practice, epoxy resin and hardener generate covalent bonds stochastically when the distance between active sites of epoxy resin and hardener is less than a certain distance; in this space two active sites can share their electrons to make potential energy stable. This is also known as the curing process in polymer science. Since the quality of the curing process affects the mechanical/thermal properties of an epoxy-based system, replicating this curing process numerically is necessary to improve reliability of the MD simulation result [36]. Details of the curing process are as follows. First, the epoxide group of DGEBF and the amine group of DETA will maintain equilibrium distances by inter/intramolecular potential energy (stage 1 of figure 2). Second, the carbon–oxygen bond in the epoxide group and nitrogen-hydrogen bond in the amine group are broken. Third, from these separations, oxygen and hydrogen atoms react to generate an O–H covalent bond (stage 2 of figure 2). Finally, the carbon of the epoxide group and nitrogen of the amine group react with each other and generate a C–N covalent bond (stage 3 in figure 2). Figure 3 shows a 3D visualization of DEGBF/DETA cross-linked systems; where red, blue, cyan and gray spheres represent nitrogen, oxygen, carbon and hydrogen atoms, respectively. In figure 3(*a*), the red dotted lines indicate that the activated carbon atoms and activated nitrogen atoms react to generate a C–N covalent bond. DETA has three nitrogen atoms and can generate five C–N covalent bonds; both end nitrogen atoms have two active sties and the middle nitrogen atom has one active site (see figures 5(*c*) and (*d*)). In addition to the C–N covalent bond between DGEBF and DETA, a photo-induced covalent bond, which is called cyclobutane, between TCE monomers should be considered. Figure 4 depicts the cyclobutane formation process, known as UV-induced [2+2] photocycloaddition, by which TCE monomers generate TCE polymers. After absorbing the UV-light energy, the equilibrium of the C=C double bonds (called cinnamoyl groups) are broken, which leads to the generation of cyclobutane. Since the numerical generation of cyclobutane is beyond the scope of this paper, the photo-induced cross-linking degree is fixed at 40%, as investigated in Oya *et al* [37]. It must be noted that in this paper a cross-linking degree means the extent of cure. In order to quantify cross-linking degree in an MD simulation, the ratio of the generated covalent bonds to the total active sites of the system is defined.

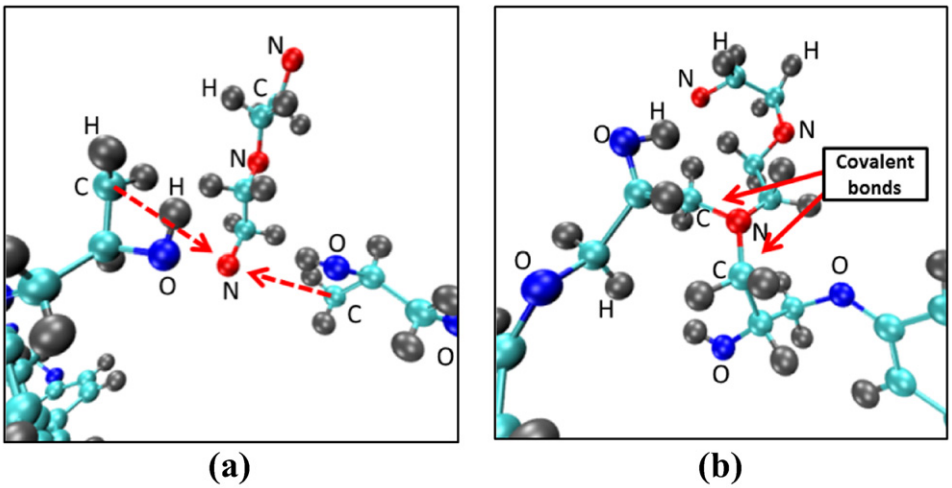

Figure 3. Schematic illustration of the molecular structure before and after covalent bond generation; gray, cyan, blue and red spheres represent hydrogen, carbon, oxygen and nitrogen, respectively. It shows that nitrogen makes two covalent bonds with two DGEBFs.

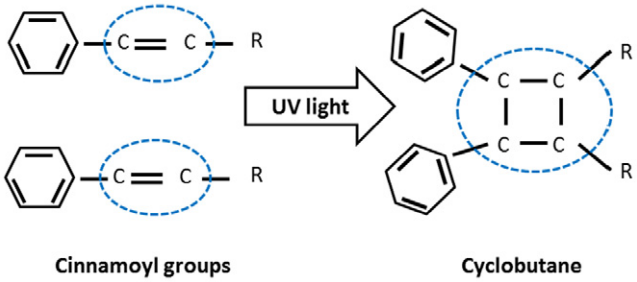

Figure 4. Schematic illustration of the procedure of cyclobutane generation in TCE monomers.

In order to replicate covalent bond generation between DGEBF and DETA in an MD simulation, activated DGEBF and DETA molecules are created by removing five hydrogen atoms from the three nitrogen atoms of DETA, and by changing the epoxide group to the methylene group as seen in figure 5. With all the activated DGEBF and DETA molecules, and 40% cross-linked TCE molecules, the smart polymer unit cell for an MD simulation is constructed. Periodic boundary conditions (PBC) are applied to the boundaries of the unit cell in all three directions (the initial size of the unit cell is approximately $7 \times 7 \times 7\,\mathrm{nm}^3$). After the initial configuration, the conjugate gradient energy minimization is performed. Next, the NPT (isobaric-isothermal) ensemble simulation is conducted to equilibrate the unit cell using the Nosé–Hoover thermostat and barostat to control the temperature and pressure at 300 K and 1 atm for 150 ps. The equilibration of the system was achieved when the potential energy showed a fluctuation around a constant mean value. Through the equilibration step, the molecules maintain minimum distances between them. Subsequently, the MD simulator generates covalent bonds when the distances between the carbon and nitrogen atoms are within

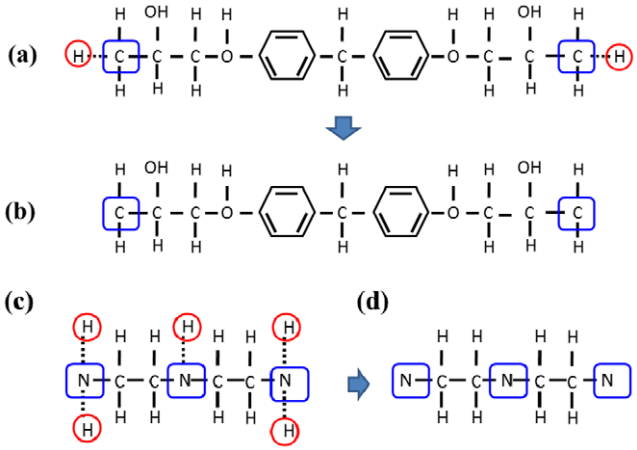

Figure 5. Chemical structures of activated DGEBF and DETA: (*a*) pre-activated DGEBF; (*b*) activated DGEBF after removing two hydrogen atoms with red circles; (*c*) pre-activated DETA; (*d*) activated DETA after removing five hydrogen atoms with red circles.

the cutoff distance of 4 Å. Due to the stochastic nature of the phenomena, there is no clearly validated cutoff distance for covalent bond generation in an MD simulation. The value of 4 Å used in this study has been widely used on various epoxy-based systems [6, 12, 14]. After generating C–N covalent bonds, hydrogen atoms are added to the activated nitrogen atoms, which failed to generate a covalent bond. With new covalent bonds being generated, the energy minimization process should be performed to reduce the undesired repulsive forces between atoms.

2.3. Estimation of the cross-linking degree

As mentioned earlier, the development of an empirical model representing the cross-linking degree of an epoxy-based system remains a critical challenge because the cross-linking mechanism is material-dependent and is a highly stochastic phenomenon [38–40]. Several numerical studies had been conducted to predict the cross-linking degree for different epoxy resin and hardener. However, very few MD simulation results could be validated with experimental results [6, 7]. In this paper, the authors suggest a purely stochastic approach to predict a most likely cross-linking degree for an epoxy-based system using MD simulations. Since this method is based on inter/intramolecular potential energy, it will be applicable to any epoxy-based system.

The methodology comprises the following three steps: (i) construct multiple unit cells with stochastic initial locations of molecules; (ii) generate numerical C–N covalent bonds for every unit cell; and (iii) find the average values of the cross-linking degree of all the unit cells. In this paper, 500 unit cells are constructed and C–N covalent bonds are generated for all the unit cells using the numerical curing process that was introduced in the previous section. After obtaining 500 cross-linking degree data, a frequency distribution is plotted as seen in figures 6(*a*) and (*b*). The calculated average cross-linking degrees are 56% for neat epoxy and 52.7% for smart polymer, which are considered to be the most likely cross-linking degrees in this paper. Based on these values, representative neat epoxy and smart polymer unit cells are constructed to validate the proposed MD simulation framework. The values of T_gs predicted

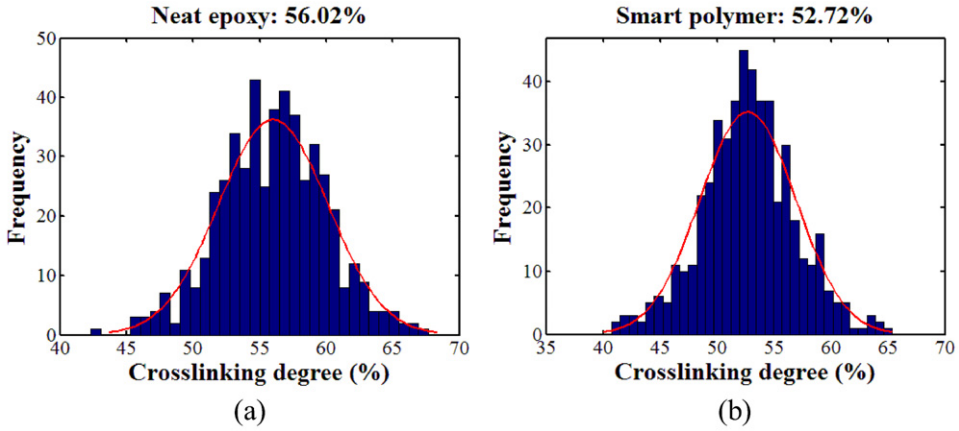

Figure 6. Most likely cross-linking degrees of neat epoxy (*a*) and smart polymer (*b*); red solid lines are fitted to the normal distributions.

by MD simulations, for both neat epoxy and smart polymer, are compared with T_gs measured by DSC. As seen in figure 6, two normal-like distributions are obtained from the histograms for both neat epoxy (mean is 56% and standard deviation is 4.1%) and smart polymer (mean is 52.7% and standard deviation is 4.2%).

2.4. Prediction of T_gs and validation of the MD simulation framework

Based on the most likely cross-linking degrees (56% for neat epoxy and 52.7% for smart polymer), T_gs have been investigated by calculating densities at temperatures ranging from 250 to 450 K. After generating covalent bonds, the system becomes unstable due to the newly generated bonds. In order to ensure the stability of the system before initiating MD simulations with different temperatures, additional energy minimization and NPT ensemble simulation (250 K and 1 atm for 200 ps) are required. With a stabilized system, a stepwise heating simulation is performed by starting with equilibrated system (250 K and 1 atm) followed by intervals of 10 K. For each temperature, an NPT ensemble simulation has been conducted for 100 ps [41]. Comparing to the experimental heating rate, 10 K/100 ps is very high; however, it is used because of the inherent timescale limitation of MD simulations [42]. To bridge the discrepancy between the experiment and simulation, an assumption made in this study is that once the system is computationally equilibrated, it will stay at the same state without any significant change and 100 ps was enough time to equilibrate the system. Densities at each temperature are calculated using the time average of densities around the equilibration state due to the fluctuation of molecules. Figures 7(*a*) and (*b*) show trends of densities as a function of temperature for neat epoxy and smart polymer. The error bars in each plot represent the MD simulation data. Since the epoxy-based systems are amorphous polymer, there is a transition in density as the temperature varies. The temperature at the transition is defined as T_g, which is determined by locating the intersection of two linearly fitted lines in the two regions: glass and liquid state region (figure 7). Through this procedure, the T_gs of neat epoxy and smart polymer are determined to be 345.2 K and 320.8 K, respectively. Table 2 shows the root mean squared error (RMSE) and R^2 to evaluate goodness-of-fit for the fitted linear curves. Since the RMSE and R^2 are close to 0 and 1, respectively, linear fit to the MD simulation results is appropriate for each region.

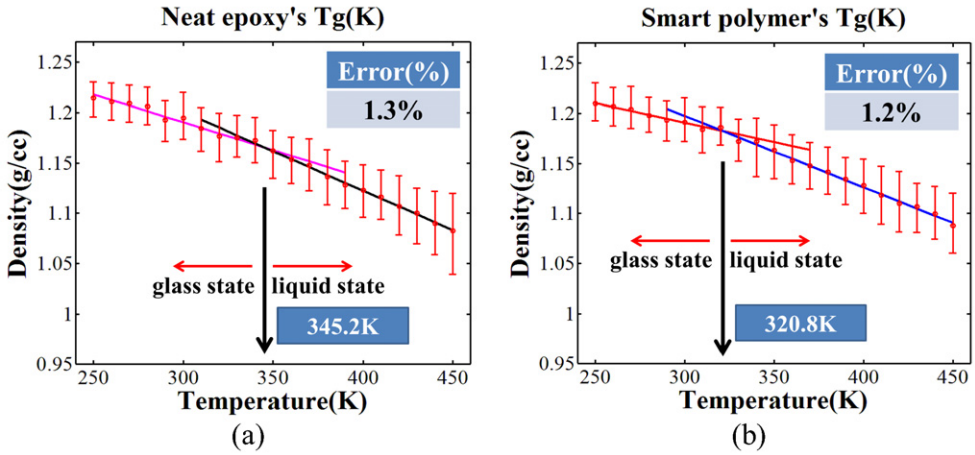

Figure 7. MD simulation results for the T_g prediction of neat epoxy (*a*) and smart polymer (*b*).

Table 2. Evaluation of goodness-of-fit.

	Neat epoxy		Smart polymer	
	Glass state	Liquid state	Glass state	Liquid state
RMSE	0.0034	0.0015	0.002	0.0023
R^2	0.97	0.99	0.96	0.99

It is necessary to validate the numerically estimated T_gs with experimental results. However, a direct comparison with data from the literature would require the construction of a molecular model of the exact material and designing the curing process corresponding to the curing condition used in the literature for that particular material. Therefore, experiments were conducted using DSC. A set of four experimental samples was fabricated for each material type: neat epoxy and smart polymer. The averaged values (from the four tests) are presented in figure 8. The comparisons between the MD simulations and DSC results are shown in table 3 which shows very good comparison of the T_g values (within 2%). These results indicate that not only does the MD simulation framework describe the epoxy-based system accurately; a combination of numerically implemented cross-linking processes and the force field MMFF is promising for epoxy-based system studies. Furthermore, the results capture the influence of the smart material on the neat epoxy; a reduction in the T_g value. Based on these results, it is anticipated that the framework developed will be a reliable numerical tool to evaluate the thermal property of any other epoxy-based system.

2.5. T_g versus cross-linking degree

Some theoretical research has been conducted on modeling the relationship between T_g and the cross-linking degree. Nielsen *et al* [43] introduced the DiBenedetto equation

$$T_g = \frac{\zeta\,\alpha\,T_{g_u} + (1-\alpha)\,T_{g_u}}{(1-\alpha) + \eta\,\alpha}, \tag{1}$$

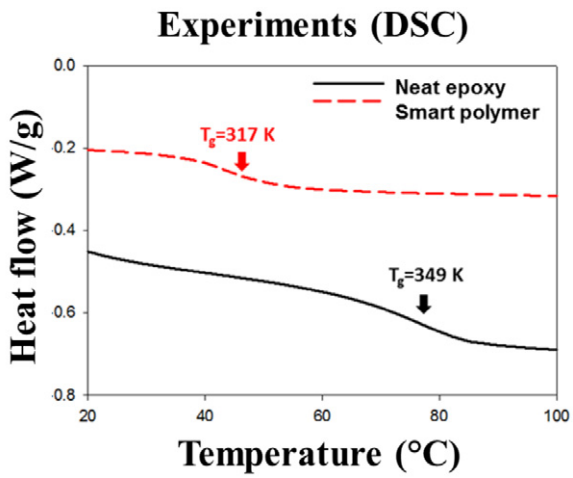

Figure 8. T_gs obtained by DSC: 349 K for neat epoxy and 317 K for smart polymer.

Table 3. Percent error of each system.

	MD simulations	DSC	% Error
Neat epoxy	345.212 K	349 K	1.3%
Smart polymer	320.801 K	317 K	1.2%

where α is the cross-linking degree ranging from 0 (uncured epoxy system) to 1 (fully cured epoxy system), ζ is the ratio of the lattice energies between an uncured epoxy system and a cured epoxy system, η is a ratio of segmental mobilities between an uncured epoxy system and a cured epoxy system and T_{g_u} is the glass transition temperature of an uncured epoxy system. Since the DibBenedetto equation does not consider the T_g of a fully cured epoxy system, it is not appropriate to use it for a highly cured system. Pascault *et al* [44] reported an extended DiBenedetto equation by introducing the T_g of fully cured epoxy system, T_{g_f},

$$T_g = \frac{(1-\alpha)T_{g_u} + \alpha\,\eta\,T_{g_f}}{(1-\alpha) + \alpha\,\eta}. \tag{2}$$

One of the well-known models is the Venditti–Gillham (V–G) equation (equation (3)) [40], which is based on an entropy approach introduced by Couchman *et al* [45],

$$T_g = \exp\left(\frac{(1-\alpha)\ln(T_{g_u}) + \alpha\,\beta\,\ln(T_{g_f})}{(1-\alpha) + \alpha\,\beta}\right), \tag{3}$$

where β is the ratio of the heat capacity change between a fully cured epoxy system and an uncured epoxy system. Venditti *et al* [40] showed comparative studies between the V–G equation and DSC measurements on several thermosetting epoxy systems, and concluded that β ranges from 0.22 to 0.65. Even though most of the β values were obtained from DSC measurements, β is not available for all thermosetting epoxy systems due to the limitations of making a fully cured or uncured epoxy system. Therefore, some β values were estimated by fitting the V–G equation to the DSC measurements of a partially cured epoxy system.

In this section, the authors use the V–G equation (equation (3)) to perform an additional validation of the MD simulation framework by fitting the V–G equation to the MD simulation data. This additional validation is meaningful because it shows that the MD simulation framework can be considered to be good tool for analyzing the relationship between T_g and

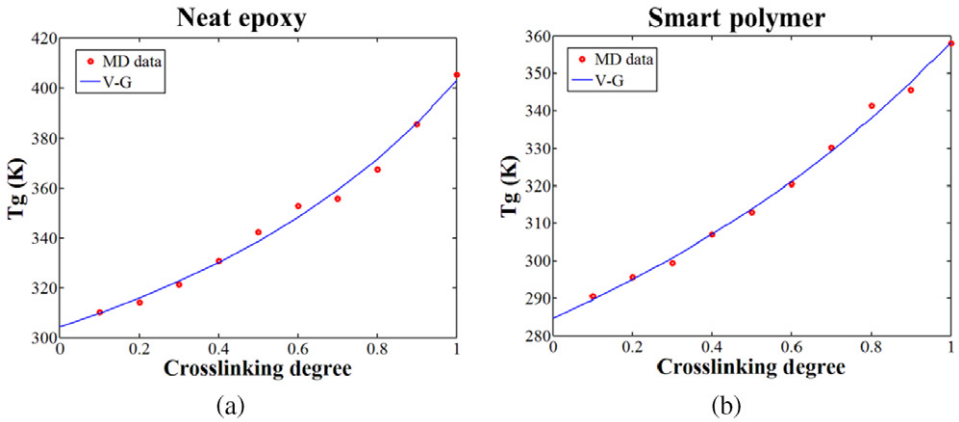

Figure 9. T_g distributions as a function of cross-linking degree, neat epoxy (a) and smart polymer (b).

Table 4. Estimated parameters by fitting V–G equation to MD data.

Material	β	$T_{g_u}(K)$	R^2
Neat epoxy	0.6164	304.3	0.9917
Smart polymer	0.7373	284.7	0.9958

the cross-linking degree, which is very important for modeling the curing mechanism of the thermoset or developing an efficient curing process. Ten different cross-linking degree unit cells (range of 10%∼100% at intervals of 10%) have been generated by tuning the cutoff distance for the curing process (section 2.2). The T_g of each unit cell has been identified by finding a kink in the temperature–density curve, which is the same method as used in section 2.4. Figure 9 shows that the MD simulation data fits well to the V–G equation for both neat epoxy and smart polymer (R^2 are 0.9917 and 0.9958, respectively, table 4). The ratio β of neat epoxy, 0.6164, is within the range mentioned in Venditti *et al* [40]. However, the ratio β of smart polymer, 0.7373, exceeds the maximum value of the range. Considering that the V–G equation was derived for neat thermoset epoxy system, the reason for the change can be attributed to the incorporation of smart material in the epoxy.

3. Conclusion

In this paper, a novel MD simulation framework has been developed to predict the cross-linking degree and the T_gs of neat epoxy and smart polymer material systems. The influence of smart material (stress-sensitive material) to the cross-linking degree and T_gs of neat epoxy has been investigated numerically and experimentally. The T_gs obtained from simulations were compared with experimental results from DSC. Considering the chemical curing process of epoxy resin and hardener, the carbon–nitrogen covalent bond generation was implemented numerically. Based on the numerical method for covalent bond generation, the cross-linking degree estimations of an epoxy-based system were conducted using a stochastic method, which made the MD simulation results more reliable. The MD-predicted T_gs of both neat epoxy and smart polymer showed excellent agreement with DSC measurement. The validity of the MD simulation framework for an epoxy-based system is established by comparing the T_g and the cross-linking

degree relation obtained by the MD simulation with the V–G equation. Furthermore, the results show that the proposed MD simulation framework captures the effect of introducing smart material to the neat epoxy, which is measured by the reduction of the T_g value. These observations will be used as guidelines in the design of smart materials with improved mechanical properties.

Acknowledgment

The authors are grateful for the support of the Air Force Office of Scientific Research (AFOSR), grant number: FA9550-12-1-0331. Dr. David Stargel is the program manager.

References

[1] Davis D A, Hamilton A and Yang J 2009 Force-induced activation of covalent bonds in mechanoresponsive polymeric materials *Nature* **459** 68–72
[2] Chen Y, Spiering A and Karthikeyan S 2012 Mechanically Induced chemiluminescence from polymers incorporating a 1, 2-dioxetane unit in the main chain *Nature Chem.* **4** 559–62
[3] Cho S, Kim J and Chung C 2008 A fluorescent crack sensor based on cyclobutane-containing crosslinked polymers of tricinnamates *Sensors Actuators* B **134** 822–5
[4] Zou J, Liu Y, Shan B, Chattopadhyay A and Dai L 2014 Early damage detection in epoxy matrix using cyclobutane-based polymers *Smart Mater. Struct.* at press
[5] Tack J L and Ford D M 2008 Thermodynamic and mechanical properties of epoxy resin DGEBF crosslinked with DETDA by molecular dynamics *J. Mol. Graph. Modelling* **26** 1269–75
[6] Varshney V, Patnaik S S and Roy A K 2008 A molecular dynamics study of epoxy-based networks: cross-linking procedure and prediction of molecular and material properties *Macromolecules* **41** 6837–42
[7] Li C and Strachan A 2010 Molecular simulations of crosslinking process of thermosetting polymers *Polymer* **51** 6058–70
[8] Nouri N and Ziaei-Rad S 2011 A molecular dynamics investigation on mechanical properties of cross-linked polymer networks *Macromolecules* **44** 5481–9
[9] Bandyopadhyay A, Valavala P K and Clancy T C 2011 Molecular modeling of crosslinked epoxy polymers: the effect of crosslink density on thermomechanical properties *Polymer* **52** 2445–52
[10] Valavala P, Odegard G and Aifantis E 2009 Influence of representative volume element size on predicted elastic properties of polymer materials *Modelling Simul. Mater. Sci. Eng.* **17** 045004
[11] Fan H B and Yuen M M 2007 Material properties of the cross-linked epoxy resin compound predicted by molecular dynamics simulation *Polymer* **48** 2174–8
[12] Yu S, Yang S and Cho M 2009 Multi-scale modeling of cross-linked epoxy nanocomposites *Polymer* **50** 945–2
[13] Choi J, Yu S and Yang S 2011 The glass transition and thermoelastic behavior of epoxy-based nanocomposites: a molecular dynamics study *Polymer* **52** 5197–203
[14] Wu C and Xu W 2006 Atomistic molecular modelling of crosslinked epoxy resin *Polymer* **47** 6004–9
[15] Liu H, Li M and Lu Z 2011 Multiscale simulation study on the curing reaction and the network structure in a typical epoxy system *Macromolecules* **44** 8650–60
[16] Chang S and Kim H 2011 Investigation of hygroscopic properties in electronic packages using molecular dynamics simulation *Polymer* **52** 3437–42
[17] Soni N J, Lin P and Khare R 2012 Effect of cross-linker length on the thermal and volumetric properties of cross-linked epoxy networks: a molecular simulation study *Polymer* **53** 1015–19
[18] Lin P and Khare R 2010 Local chain dynamics and dynamic heterogeneity in cross-linked epoxy in the vicinity of glass transition *Macromolecules* **43** 6505–10
[19] Lin P and Khare R 2010 Glass transition and structural properties of glycidyloxypropyl-heptaphenyl polyhedral oligomeric silsesquioxane–epoxy nanocomposites *J. Therm. Anal. Calorim.* **102** 461–7
[20] Lin P and Khare R 2009 Molecular simulation of cross-linked epoxy and epoxy-POSS nanocomposite *Macromolecules* **42** 4319–27

[21] Li C and Strachan A 2011 Effect of thickness on the thermo-mechanical response of free-standing thermoset nanofilms from molecular dynamics *Macromolecules* **44** 9448–54
[22] Brooks B R, Bruccoleri R E and Olafson B D 1983 CHARMM: a program for macromolecular energy, minimization, and dynamics calculations *J. Comput. Chem.* **4** 187–217
[23] Yang S, Yu S, Ryu J, Cho J M, Kyoung W, Han D S and Cho M 2013 Nonlinear multiscale modeling approach to characterize elastoplastic behavior of CNT/polymer nanocomposites considering the interphase and interfacial imperfection *Int. J. Plast.* **41** 124–146
[24] Halgren T A 1996 Merck molecular force field: I. Basis, form, scope, parameterization, and performance of MMFF94 *J. Comput. Chem.* **17** 490–519
[25] Halgren T A 1996 Merck molecular force field: II. MMFF94 van der Waals and electrostatic parameters for intermolecular interactions *J. Comput. Chem.* **17** 520–52
[26] Halgren T A 1996 Merck molecular force field: III. Molecular geometries and vibrational frequencies for MMFF94 *J. Comput. Chem.* **17** 553–86
[27] Halgren T A and Nachbar R B 1996 Merck molecular force field: IV. Conformational energies and geometries for MMFF94 *J. Comput. Chem.* **17** 587–615
[28] Halgren T A 1996 Merck molecular force field: V. Extension of MMFF94 using experimental data, additional computational data, and empirical rules *J. Comput. Chem.* **17** 616–41
[29] Plimpton S 1995 Fast parallel algorithms for short-range molecular dynamics *J. Comput. Phys.* **117** 1–19
[30] Liu Y, Fard M Y and Chattopadhyay A 2012 Damage assessment of CFRP composites using a time–frequency approach *J. Intell. Mater. Syst. Struct.* **23** 397–413
[31] Tou W I, Chang S S, Lee C C and Chen C Y C 2013 Drug design for neuropathic pain regulation from traditional Chinese medicine *Sci. Rep.* **3** 844
[32] Ericksen S S, Cummings D F and Teer M E 2012 Ring substituents on substituted benzamide ligands indirectly mediate interactions with position 7.39 of transmembrane helix 7 of the D4 dopamine receptor *J. Pharmacol. Exp. Therapeutics,* **342** 472–85
[33] Shim J and MacKerell A D Jr 2011 Computational ligand-based rational design: role of conformational sampling and force fields in model development MedChemComm **2** 356–70
[34] Allen F H 2002 The Cambridge structural database: a quarter of a million crystal structures and rising *Acta Crystallogr.* B **58** 380–8
[35] Zoete V, Cuendet M A and Grosdidier A 2011 SwissParam: a fast force field generation tool for small organic molecules *J. Comput. Chem.* **32** 2359–68
[36] Ellis B 1993 *Chemistry and Technology of Epoxy Resins* (London: Blackie Academic & Professional)
[37] Oya N, Sukarsaatmadja P and Ishida K 2012 Photoinduced mendable network polymer from poly (butylene adipate) end-functionalized with cinnamoyl groups *Polym. J.* **44** 724–9
[38] Aronhime M T and Gillham J K 1986 *Epoxy Resins and Composites III* (Berlin: Springer) pp 83–113
[39] Enns J B and Gillham J K 1983 Time–temperature-transformation (TTT) cure diagram: modeling the cure behavior of thermosets *J. Appl. Polym. Sci.* **28** 2567–91
[40] Venditti R and Gillham J 1997 A relationship between the glass transition temperature (T_g) and fractional conversion for thermosetting systems *J. Appl. Polym. Sci.* **64** 3–14
[41] Fox J R and Andersen H C 1984 Molecular dynamics simulations of a supercooled monatomic liquid and glass *J. Phys. Chem.* **88** 4019–27
[42] Buehler M J, Hartmaier A and Gao H 2004 Atomic plasticity: description and analysis of a one-billion atom simulation of ductile materials failure *Comput. Methods Appl. Mech. Eng.* **193** 5257–82
[43] Nielsen L E 1969 Cross-linking-effect on physical properties of polymers *J. Macromol. Sci. Polymer Rev* 3(1) 69–103
[44] Pascault J and Williams R 1990 Glass transition temperature versus conversion relationships for thermosetting polymers *J. Polym. Sci.* B **28** 85–95
[45] Couchman P and Karasz F 1978 A classical thermodynamic discussion of the effect of composition on glass-transition temperatures *Macromolecules* **11** 117–19